RESEARCH ARTICLE

Myocardin-related transcription factor's interaction with serum-response factor is critical for outgrowth initiation, progression, and metastatic colonization of breast cancer cells

David Gau[1] | Pooja Chawla[1] | Ian Eder[1] | Partha Roy[1,2]

[1]Department of Bioengineering, Pittsburgh, Pennsylvania, USA

[2]Department of Pathology at the University of Pittsburgh, Pittsburgh, Pennsylvania, USA

Correspondence
Partha Roy, Department of Bioengineering, 306 CNBIO, University of Pittsburgh, 300 Technology Drive, Pittsburgh, PA 15219, USA.
Email: partha.roy@pitt.edu; par19@pitt.edu

Abstract

Breast cancer (BC)-related mortality primarily results from metastatic colonization of disseminated cells. Actin polymerization plays an important role in driving post-extravasation metastatic outgrowth of tumor cells. This study examines the role of myocardin-related transcription factor (MRTF)/serum-response (SRF), a transcription system well known for regulation of cytoskeletal genes, in metastatic colonization of BC cells. We demonstrated that co-depletion of MRTF isoforms (MRTF-A and MRTF-B) dramatically impairs single-cell outgrowth ability of BC cells as well as retards growth progression of pre-established BC cell colonies in three-dimensional (3D) cultures. Conversely, overexpression of MRTF-A promotes initiation and progression of tumor-cell outgrowth in vitro, primary tumor formation, and metastatic outgrowth of seeded BC cells in vivo, and these changes can be dramatically blocked by molecular disruption of MRTF-A's interaction with SRF. Correlated with the outgrowth phenotypes, we further demonstrate MRTF's ability to augment the intrinsic cellular ability to polymerize actin and formation of F-actin-based protrusive structures requiring SRF's interaction. Pharmacological proof-of-concept studies show that small molecules capable of interfering with MRTF/SRF signaling robustly suppresses single-cell outgrowth and progression of pre-established outgrowth of BC cells in vitro as well as experimental metastatic burden of BC cells in vivo. Based on these data, we conclude that MRTF activity potentiates metastatic colonization of BC cells and therefore, targeting MRTF may be a promising strategy to diminish metastatic burden in BC.

KEYWORDS
breast cancer, CCG-1423, metastasis, MRTF, outgrowth, SRF

Abbreviations: MRTF, myocardin-related transcription factor; SRF, Serum-response factor; MoT, Matrigel-on-top; BC, breast cancer; KD, knockdown; ER, estrogen receptor; PR, progesterone receptor; HER2, human epidermal growth factor receptor 2; TNBC, triple-negative breast cancer.

1 | INTRODUCTION

The vast majority of breast cancer (BC)-related deaths are due to metastatic spread of tumor cells to distant organs. Tumor metastasis is a complex cascade of events that involves stromal invasion and intravasation of malignant sub-population of cancer cells at the primary tumor site followed by arrest of tumor cells in the vasculature, extravasation, and finally outgrowth of tumor cells at select ectopic organs. The fate of disseminated tumor cells at the ectopic site is a critical determinant of the clinical outcome of BC patients. Extravasated tumor cells can undergo dormancy for a considerable length of time, and it is the switch from dormancy-to-proliferative state that leads to the formation of micro-metastases which ultimately progress to clinically detectable macro-metastases causing mortality of cancer patients.[1,2] In principle, survival of BC patients should be improved if metastatic burden can be reduced by either prolonging the dormancy of disseminated BC cells or reverting proliferating metastases to dormancy or slowing down the metastatic growth.

Transcriptional complex formed by serum-response factor (SRF) and its cofactor myocardin-related transcription factor (MRTF) plays a key role in orchestrating signal-induced gene regulation programs controlling the expressions of a wide range of genes including those involved in cytoskeletal regulation, cell adhesion, and ECM remodeling.[3–6] The two main isoforms of MRTF in non-muscle cells are MRTF-A (also known as MKL1 or BSAC or MAL) and MRTF-B (or MKL2). In quiescent cells, MRTFs are mostly sequestered in the cytoplasm through its interaction with monomeric actin (G-actin). Fluctuation in the F-to-G-actin ratio in favor of actin polymerization liberates MRTFs from G-actin allowing MRTFs to accumulate in the nucleus and activate SRF-mediated transcription of genes including SRF itself.[7–15] MRTF-A overexpression promotes mammary epithelial cell proliferation, induction of EMT (epithelial-to-mesenchymal transition)-associated genes, and interferes with anoikis.[16] In tail-vein experimental metastasis model, knockdown (KD) of either MRTF isoforms or SRF in MDA-MB-231 (MDA-231) triple-negative BC (TNBC-negative for expression of ER [estrogen receptor], PR [progesterone receptor], and HER2) as well as in B16F1 melanoma cell lines dramatically reduced their lung colonization abilities in mice.[17] However, since metastatic colonization is impacted by a number of factors including tumor cell survival in the circulation, extravasation, metastatic seeding, and proliferation, the underlying basis for defect in metastatic colonization induced by loss of MRTF function is unclear. MRTF gene signature is elevated in tumor cells at the perivascular niche in an organotypic brain-colonization model of lung cancer.[18] These findings, taken together with recent demonstrations of MRTF's ability to sensitize BC cells to immune surveillance and eliminate tumor cells from metastatic site at high expression level,[19] further suggest MRTF's complex role in the regulation of metastatic colonization of tumor cells.

Although SRF activation is one of its major functions, MRTF is also capable of regulating gene transcription utilizing its SAP domain (a putative chromatin-binding domain) in an SRF-independent manner.[20,21] Conversely, SRF can be also activated through its interaction with ternary complex factor (TCF) family of co-activators that leads to transcription of genes distinct from those initiated by MRTF's action.[22] Therefore, the role of MRTF-SRF interaction in particular in metastatic colonization of tumor cells cannot be extrapolated from previously reported findings in KD setting of either MRTF or SRF.[17] In this study, we demonstrate critical importance of MRTF-SRF interaction in promoting outgrowth initiation, progression, and metastatic colonization of BC cells, and proof-of-concept for pharmacological intervention of MRTF/SRF activity as an impactful strategy to diminish metastatic burden of BC cells.

2 | MATERIALS AND METHODS

2.1 | Cell culture and transfection

MDA-MB-231 (MDA-231) cells, either parental or a subline that stably co-expresses mCherry and luciferase (a gift from Dr. Jennifer Koblinski, Virginia Commonwealth University), HEK-293 (ATCC, catalog # CRL-1573), and MDA-468 (ATCC, catalog # HTB-132) were cultured in DMEM media (Lonza, catalog# BW12-604F) supplemented with 10% (v/v) fetal bovine serum (FBS; Corning, catalog# MT35011CV) and antibiotics (100 U/ml penicillin and 100 μg/ml streptomycin; Thermo Fisher, catalog# 15070063). Luciferase-expressing sublines of 4T1 (a gift from Dr. Carolyn Anderson, University of Missouri) and D2A1 (a gift from Dr. William Schiemann, Case Western Reserve University) cell lines, T47D (ATCC, catalog# HTB-133), BT474 (ATCC, catalog# HTB-20), MCF7 (ATCC, catalog# HTB-22), and SKBR3 (ATCC, catalog# HTB-30) cells were cultured in RPMI media (Lonza, catalog # BW12702F) supplemented with 10% (v/v) FBS and antibiotics (100 U/ml penicillin and 100 μg/mL streptomycin). The lentiviral vectors used to express doxycycline (DOX)-inducible wild-type (WT)-MRTF-A, ΔSAP-MRTF-A (lacks SAP-domain), or ΔSRF-MRTF-A (harbors point-mutations that disrupt MRTF-SRF interaction––details

described in Section 3), and MRTF-B in stably expressing GFP-Luc MDA-231 cells were constructed and packaged by VectorBuilder. Vector IDs (VB200831-1118ktq, VB200831-1115pnv, VB200831-1117jwj, and VB200825-1202ewr) can be used to retrieve detailed information about the vectors on vectorbuilder.com. For silencing of genes, smart-pool MRTF-A siRNA (Santa Cruz, catalog #sc-43944) and MRTF-B siRNA (Santa Cruz, catalog #sc-61074) were transfected at 2.5–5 nM concentration with Lipofectamine RNAiMAX (Thermo Fisher, catalog #13778100) following the manufacturer's instructions. CCG-1423 was purchased from Santa Cruz (catalog #sc-205241). CCG-203971 was a product of Cayman Chemicals (catalog #15075).

2.2 | Matrigel-on-top (MoT)

Three-dimensional outgrowth of BC cells was assessed using MoT assay in a 96-well format as previously described.[23–25] Briefly, depending on the cell line, 2000–5000 cells were seeded in triplicates in a 96-well plate on a layer of 100% growth factor-reduced Matrigel (Cultrex, Trevigen, catalog #3445–010-01) and then overlaid with culture media and 2% Matrigel that was changed every other day. For CCG-related experiments, unless indicated otherwise, cells were plated as described, and treated with either DMSO or CCG every other day with media changes. After 7–10 days of culture, cells were imaged at 4× magnification to capture most of the well using an Olympus IX71 microscope, and outgrowth was quantified by the total area of the colonies using ImageJ. The absolute value of tumor cell outgrowth in MoT assay varies due to batch-to-batch variability of Matrigel and subtle changes in the culture media composition from experiment-to-experiment. Therefore, for a given biological replicate of experiments, the outgrowth readout for each well in the technical replicates of the experimental group was normalized to the average outgrowth readout of the control group. These ratios were then averaged over the number of biological replicates to calculate the mean and standard deviation of the outgrowth of the experimental group relative to the control group.

2.3 | Cell viability

BC cells were stained using a live/dead assay kit (Thermo Fisher, catalog #L3224) following manufacturer's instructions after MoT assay or overnight treatment of CCG compound as previously described.[26] Stained cells were imaged with at 4× magnification.

2.4 | Protein extraction and immunoblotting

Cell lysates were prepared by a modified RIPA buffer (25 mM Tris–HCL: pH 7.5, 150 mM NaCl, 1% (v/v) NP-40, 5% (v/v) glycerol), 1 mM EDTA, 50 mM NaF, 1 mM sodium pervanadate, and protease inhibitors (Sigma, catalog P8340) supplemented with 6× sample buffer diluted to 1× with the final SDS concentration in the lysis buffer equivalent to 2%. Primary tumor lysates were prepared by homogenizing tumor or comparable mass of mammary fat pad (when tumor size was negligible) in modified RIPA buffer. Lysates were then supplemented with 6× sample buffer diluted to 1× with the final SDS concentration in the lysis buffer equivalent to 2%. Conditions for the various antibodies were: polyclonal MRTF-A (Cell Signaling, catalog #14760S; 1:1000), MRTF-B (Cell Signaling, catalog #14613S; 1:1000) monoclonal SRF (Active Motif, catalog #61385, 1:1000), polyclonal GAPDH (Sigma, catalog #G9545, 1:2000), polyclonal CTGF (Abcam, catalog #ab6992), monoclonal mCherry (Fisher Scientific, catalog #M11217, 1:1000), polyclonal anti-rat HRP (VWR, catalog # 10147–312, 1:1000), monoclonal anti-rabbit HRP (Jackson Immunoresearch, catalog #211–032-171, 1:1000), and polyclonal anti-mouse HRP (BD Biosciences, catalog #554002, 1:1000).

2.5 | Cell proliferation in 2D culture

Five-thousand MDA-231 cells were plated in the wells of a 24-well plate in triplicates on day 0 and cultured overnight before being subjected to either 10 μM CCG-1423 or vehicle treatment on day 1. Cells were trypsinized and counted on day 4. The medium was replenished every other day with the appropriate treatment.

2.6 | F-Actin staining

Cells cultured on either coverslips or matrigel were washed with DPBS (Lonza, catalog #BW17513F) and fixed with 3.7% formaldehyde (2D culture—15 min; 3D culture—30 min). Following permeabilization with 0.5% Triton X-100 for 5 min, cells were stained with ~33 nm phalloidin, conjugated with either rhodamine (Life Technologies, catalog #R415) or far-red (Cytoskeleton Inc, catalog #PHDN1-A) fluorophore, for 20 min at room temperature. Stained cells were washed twice with PBS containing 0.02% Tween 20, twice with PBS, and once with distilled water before being mounted on a slide and imaged with a ×60 oil immersion objective for coverslips

(N.A. = 1.4) or ×40 objective for matrigel on an Olympus IX-71 inverted microscope. The same constant threshold was set between all fields with parameters that prevented overexposure; cell size and the average fluorescence intensity were scored on a cell-by-cell basis by manual tracing using ImageJ.

2.7 | Animal studies

All animal experiments were conducted in compliance with an approved IACUC protocol, according to University of Pittsburgh Division of Laboratory Animal Resources guidelines. For experimental metastasis studies involving CCG-1423, 4T1-Luc (1×10^5 cells) cells were suspended in 100 μl PBS and injected into the left cardiac ventricle of anesthetized 6-week-old female BALB/c mice (Source: Jackson Laboratory) using a 29G syringe needle. Since BC is much more prevalent in female, only female mice were used in our studies. Mice were injected daily with CCG-1423 (3 mg/kg) or DMSO (vehicle control) via intraperitoneal route starting immediately after intracardiac injection for 7–10 days until sacrifice. To evaluate the effect of overexpression of WT versus functional mutants of MRTF-A on experimental metastasis of BC cells, 1×10^5 cells GFP+/Luc + MDA-231 cells engineered for DOX-inducible expression of various MRTF-A constructs or empty vector (EV) as control were suspended in 100 μl PBS and injected into the left cardiac ventricle of anesthetized 6-week-old female NOD *scid* gamma (NSG) mice (Source: Jackson Laboratory). Mice were provided with water supplemented with DOX (2 mg/ml with 5% sucrose) to induce and maintain expression of MRTF-A constructs in vivo. Bioluminescence imaging (BLI) of anesthetized mice was acquired with IVIS Spectrum at 15 min after intraperitoneal injection of D-luciferin (50 mg/kg; PerkinElmer, catalog #122799). Images were analyzed by Living Image 4.3 software (PerkinElmer). Hematoxylin and Eosin (H&E) staining of bone sections (utilizing the service provided by the histology core) were performed for orthogonal confirmation of bone metastases. For orthotopic xenograft studies, 1×10^6 GFP+/Luc + MDA-231 cells belonging to the various sublines were reconstituted in 50 μl of 1:1 PBS/matrigel mix and were inoculated into the fourth inguinal mammary fat pad of anesthetized 5–6 week-old female NSG mice and tumor growth was monitored.

2.8 | Quantitative RT-PCR

Total RNA was extracted from cultured cells from MoT assay (scaled up a six-well-setting) using RNeasy mini kit (Qiagen, catalog #74104) according to the manufacturer's

instructions. Complementary DNA (cDNA) was synthesized from 1 μg of RNA using the Quantitect reverse transcription kit (Qiagen, catalog #205311) following the manufacturer's instructions. Each PCR was prepared with 50 ng of cDNA, 12.5 μl of SYBR Select Master Mix (Thermo Fisher, catalog #4472903), 1 μM (final concentration) forward and reverse primers, and water for a total volume of 25 μl. Thermal cycling and data analysis were performed using the StepOne Plus Real-Time PCR System and StepOne Software (Applied Biosystems) to detect quantitative mRNA expression of CTGF and GAPDH (endogenous control). The primer sequences for GAPDH were 5′-CGGAGTCAACGGATTTGGTCGTAT-3′ (sense) and 5′-AGGCTTCTCCATGGTGGTGAAGAC-3′ (antisense). The primer sequences for CTGF were 5′-GCAGGCTAGAGAAGCAGAGC-3′ (sense) and 5′-GGTGCAGCCAGAAAGCTC-3′ (antisense). The PCR cycling conditions for GAPDH and CTGF were 95°C (30 s), 55°C (30 s), and 72°C (1 min) for a total of 40 cycles.

2.9 | Statistics

When comparing two groups for in vitro studies, we performed either student *t*-test or a nonparametric *t*-test (Mann–Whitney). For multiple group comparisons, we used ANOVA followed by Tukey post hoc test. For in vivo multiple group comparisons, we used ANOVA followed by Tamhane's T2 non-equal variance post hoc test. A $p < 0.05$ was considered statistically significant.

3 | RESULTS

3.1 | MRTF depletion suppresses single-cell outgrowth of BC cells in 3D culture

Because of the complex nature of the in vivo environment, many important biological insights underlying post-extravasation behavior of BC cells were previously elucidated from experiments utilizing widely used Matrigel-on-Top (MoT) assay. This assay measures single-cell outgrowth competency of BC cells in a 3D culture environment and accurately predicts their lung colonization competency in vivo.[25,27–29] To determine whether MRTF plays an important role in single-cell outgrowth of BC cells, we first assessed the effect of transient co-silencing of MRTF isoforms on single-cell outgrowth behavior of both ER-positive (ER+) and ER-negative (ER−) BC cells in MoT assays. Specifically, we performed these studies using human T47D luminal-A (ER+) BC and MDA-231 TNBC cell lines. Immunoblots in Figure 1A demonstrates
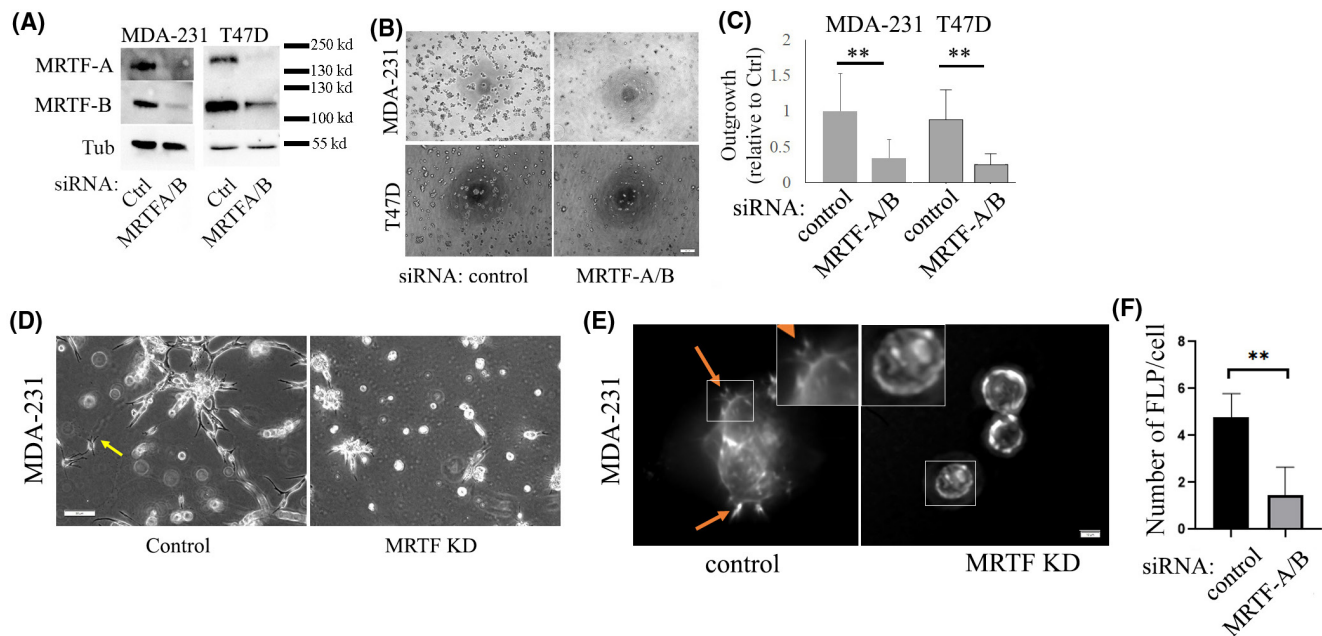
FIGURE 1 Effect of silencing of myocardin-related transcription factor (MRTF) on single-cell outgrowth of breast cancer cells in MoT assay. (A) Representative immunoblots of MRTF-A and MRTF-B from the extracts of MDA-231 andT47D cells transfected with the indicated siRNAs (tubulin blot––loading control). (B) Representative images of outgrowth of MDA-231 and T47D cells treated with the indicated siRNAs. (C) A bar graph summarizing the relative outgrowth of MRTF-silenced culture compared to control siRNA-transfected culture (summarized from three independent experiments). (D–F) Representative phase-contrast images (panel D; scale bar—200 μm) and fluorescence images of phalloidin-stained cells (panel E; scale bar 10 μm) showing morphological changes and defect in FLP formation (arrows) caused by MRTF depletion in MDA-231 cells in 3D culture. The insets show magnified images of the regions of interest outlined by squares. The bar graph in panel F summarizes the average number of FLP per cell of control versus MRTF-depleted cells. Values are presented as mean ± SD summarized from two independent experiments with at least 20 cells analyzed from each group (**$p < 0.01$)

successful KD of MRTF-A and MRTF-B in these cell lines. Co-depletion of MRTFs led to a significant impairment in 3D outgrowth of both MDA-231 and T47D cells (Figure 1B,C). MRTF-deficient cells were either arrested at a single-cell stage or failed to progress beyond a cluster of few cells during the period of observation suggesting induction of a dormancy-like response in these BC cell lines. Metastatic outgrowth of extravasated BC cells is critically dependent upon early changes in actin cytoskeletal architecture marked by formation of F-actin-rich filopodial protrusions (FLP) and contractility-driven assembly of actin stress-fibers (SFs). These cytoskeletal structures enable activation of a proliferation-inducing signaling axis initiated by cell-ECM adhesion in disseminated BC cells leading to metastatic outgrowth. Failure to initiate FLP and actin SF assembly induces dormancy in disseminated BC cells in vitro (in MoT assay) and in vivo.[25,27–29] We noticed morphological differences between 3D cultures of control and MRTF-KD MDA-231 cells. While control cells formed robust protrusive structures and displayed elongated phenotype, MRTF KD cells predominantly assumed round morphology with clear evidence for a defect in forming protrusive structures (Figure 1D). Correlated with these phenotypes, phalloidin staining further revealed that KD

of MRTFs induces defects in FLP formation in 3D culture as indicated by a prominent reduction in average FLP count/cell in MRTF KD relative to the control group (Figure 1E,F). Collectively, these data demonstrate that actin organization, cellular morphology, and outgrowth ability of BC cells are sensitive to loss of MRTF.

3.2 | MRTF-A overexpression promotes single-cell outgrowth as well as progression of pre-established outgrowth of BC cells in 3D culture requiring both SRF's interaction and SAP-domain function

Next, to determine the impact of overexpression of MRTF on single-cell outgrowth, we engineered sublines of GFP/luciferase (Luc)-expressing MDA-231 cells for stable DOX-induced overexpression of either wild-type MRTF-A (denoted as WT-MRTF-A) or mutant constructs of MRTF-A, with empty vector transduced cells serving as control. Mutant constructs of MRTF-A were either impaired in binding to SRF (through introducing previously described K237A/Y238A/H239A/Y241A point

mutations in the basic-rich B1 domain [21]—referred to as ΔSRF-MRTF-A hereon) or lacked the entire SAP-domain (referred to as ΔSAP-MRTF-A hereon) (see Figure 2A for a structural schematic of MRTF showing its various functional domains). Since commonly used BC cell lines with metastatic propensity in experimental settings are generally TN in nature, we focused on MDA-231 TN cell line as our main model cell line for majority of our experiments. Immunoblot data in Figure 2B shows the relative expressions of the various MRTF-A constructs in

these sublines of MDA-231 cells. Since SRF is also transcriptionally regulated by the MRTF/SRF complex, cells overexpressing either MRTF-A or ΔSAP-MRTF-A but not ΔSRF-MRTF-A had higher level of SRF relative to control as expected (Figure 2B). Consistent with our KD experimental results, overexpression of WT-MRTF-A-stimulated single-cell outgrowth of MDA-231 cells in 3D culture (Figure 2C,D). Likewise, stable overexpression of MRTF-B also enhanced the outgrowth ability of MDA-231 cells in MoT assay (Figure S1). While overexpression of
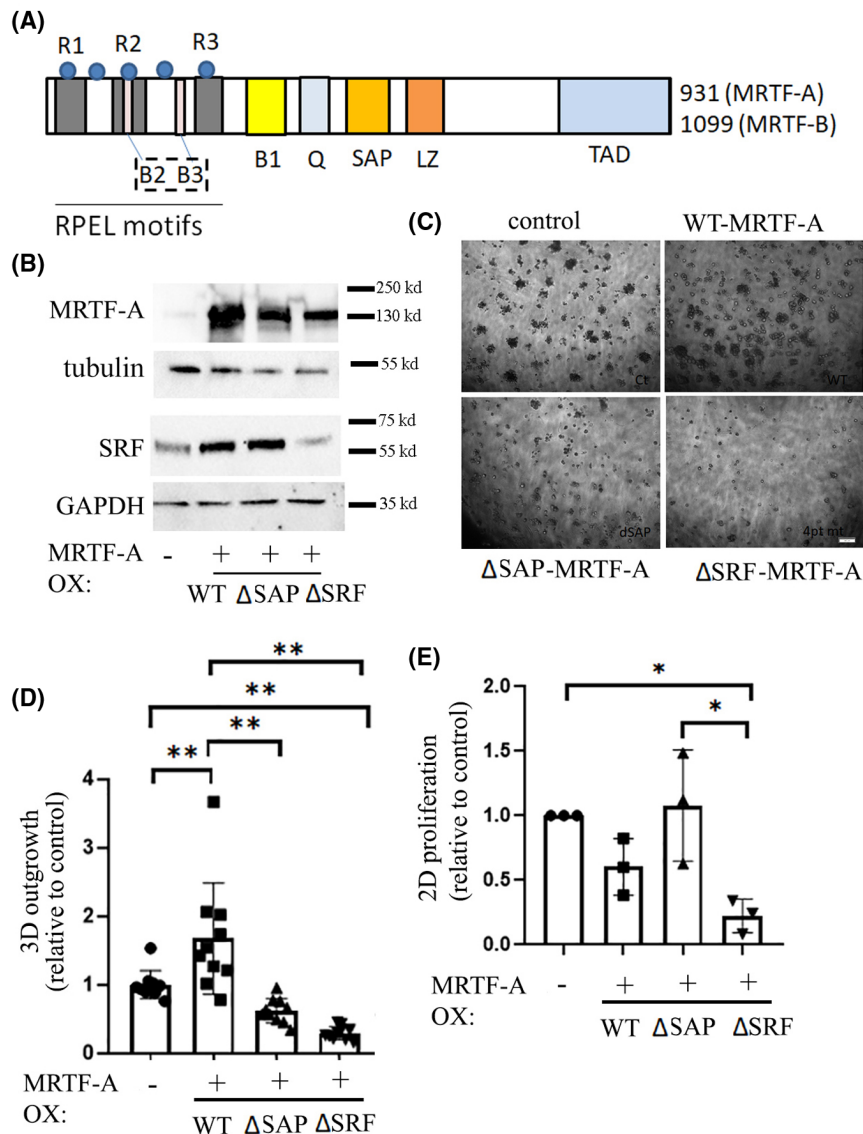

FIGURE 2 Effect of overexpression of wild-type versus functional mutants of MRTF-A on single-cell outgrowth of breast cancer cells in MoT assay. (A) Structural schematic of MRTF: Actin-binding (RPEL: R1, R2, R3), basic-rich (B1 [SRF-binding], B2, B3), glutamine-rich (Q), putative chromatin-binding (SAP), dimerization-inducing leucine-zipper (LZ), and transcriptional activation (TAD) domains––Numbers denote the last amino acid of human MRTF isoforms. (B) Immunoblot showing doxycycline (DOX)-inducible stable overexpression (OX) of indicated MRTF-A constructs and associated changes in SRF level in GFP/luciferase (luc) expressing MDA-231 cells (tubulin and GAPDH blots serve as the loading controls for MRTF-A and SRF, respectively). (C, D) Representative images (panel C) and quantification (panel D) summarizing single-cell 3D outgrowth of the indicated MRTF-A expressing sublines of MDA-231 cells in MoT assay. (E) A comparison of the proliferation of the same sublines in 2D cell culture. All data are summarized from three independent experiments (*$p < 0.05$; **$p < 0.01$). Values are presented as mean ± SD (**$p < 0.01$). Scale bar represents 200 μm

either of the two mutants of MRTF-A failed to elicit this change, ΔSRF-MRTF-A expressers displayed the most dramatic outgrowth-deficient phenotype with many cells arrested at single-cell stage (a characteristic of dormancy-like phenotype). Reduced outgrowth competency of ΔSRF-MRTF-A expressers relative to control cells is suggestive of a dominant-negative action of this mutant, a feature that is expected because MRTFs homo- and hetero-dimerize. Interestingly, only ΔSRF-MRTF-A but not ΔSAP-MRTF-A expressers exhibited proliferation defect in rigid 2D tissue-culture substrate (Figure 2E), possibly suggesting that substrate stiffness may dictate the requirement for the SAP-domain function in tumor cell proliferation.

To determine how actin cytoskeleton is impacted by functional disruptions of MRTF, we performed phalloidin staining of the various sublines of MDA-231 cells in either 2D or 3D MoT culture. Overexpression of either WT-MRTF-A or ΔSAP-MRTF-A but not ΔSRF-MRTF-A led to a prominent increase in the overall level of polymerized actin including induction of actin stress-fibers in 2D culture (Figure 3A,B). In 3D culture, control cells exhibited FLP structures (denoted by blue arrows) as expected (Figure 3C). While both WT-MRTF-A and ΔSAP-MRTF-A expressers exhibited stronger F-actin staining than control cells, these two sublines formed strong F-actin clusters (denoted by yellow arrows) instead of exhibiting FLPs, a feature that was also completely absent in ΔSRF-MRTF-A expressing cells. These data underscore the importance of MRTF-SRF interaction in determining the overall cellular ability to polymerize actin and formation of various actin-based structures in BC cells.

To further investigate whether perturbing MRTF alters the growth progression of pre-established tumor-cell colonies (an in vitro mimic of micro- to macro-metastasis progression), we seeded control, WT-, and mutant-MRTF-A overexpressing MDA-231 cells in MoT culture initially in an uninduced state (i.e., without pre-exposure to DOX). We then allowed these cells to outgrow for 7 days to establish small colonies before triggering the expressions of the various transgenes by DOX and measuring the end-point outgrowth on day 14. Based on comparable levels of MRTF-A expression between these various sublines even after 1 month of culture without exposure to DOX in pilot experiments, we were able to confirm that there is no leaky expression of the transgenes in the absence of DOX exposure (Figure S2). Our experiments showed comparable outgrowth of various groups of cells on day 7 as expected but triggering of WT-MRTF-A overexpression accelerated the subsequent growth, which was abrogated by disruption of either SRF's interaction or SAP-domain function (Figure 4). Between the two mutants, ΔSRF-MRTF-A had the strongest growth suppressive effect when

overexpressed. Collectively, these results demonstrate that MRTF accelerates single-cell outgrowth as well as progressive growth of BC cells requiring its SRF's interaction and SAP-domain functions with stronger dependence on its SRF interaction.

3.3 | MRTF-SRF interaction is critical for metastatic growth of BC cells in vivo

To determine the consequence of selective disruption of SRF's interaction and SAP-domain functions of MRTF on metastatic colonization of BC cells in vivo, we performed experimental metastasis assays with the various sublines of MDA-231 cells in immunodeficient NOD-*scid*-gamma (NSG) mice. We preferred intracardiac injection (ICI) over tail-vein injection model because unlike tail-vein injection model where metastasis is restricted to lungs only, ICI-based experimental assay leads to wide-spread metastases including in mechanically stiffer organs (such as bones) which has not been explored in previous studies involving MRTFs. We performed two sets of experimental metastasis experiments. In our first set of experiments, overexpression of the various MRTF-A constructs were pre-induced by DOX treatment before tumor cells were inoculated in mice and the transgene expression was maintained until the end of the experiment by feeding animals with DOX (2 mg/ml)-supplemented water (schematically shown in Figure 5A). The metastatic burden was longitudinally monitored until sacrifice by bioluminescence imaging [BLI] and quantified either by overall (whole animal) BLI signal readout or distant BLI readout (farther away from chest region) where we specifically focused our regions of interest in the head and lower extremities (representative images of end-point BLI images for various groups are shown in Figure 5B). Regardless of the method of quantification, animals inoculated with WT-MRTF-A overexpressing cells exhibited much higher mean BLI readout than control animals, and the mean BLI signal of those bearing ΔSRF-MRTF-A expressers was found to be significantly lower than even control animals (Figure 5C). Although the overall BLI signal of animals bearing ΔSAP-MRTF-A expressers was lower than those inoculated with WT-MRTF-A expressers ($p = 0.09$—failure to reach statistical significance likely stems from large standard deviation of the latter group), the distant BLI readouts of these groups were not different ($p = 0.63$). These data suggest MRTF-SRF interaction plays a key role in development of distant metastases from circulating tumor cells.

Since our foregoing experiments cannot discern whether MRTF promotes development of metastases from circulating cells by affecting survival of tumor cell in circulation and/or extravasation and/or early
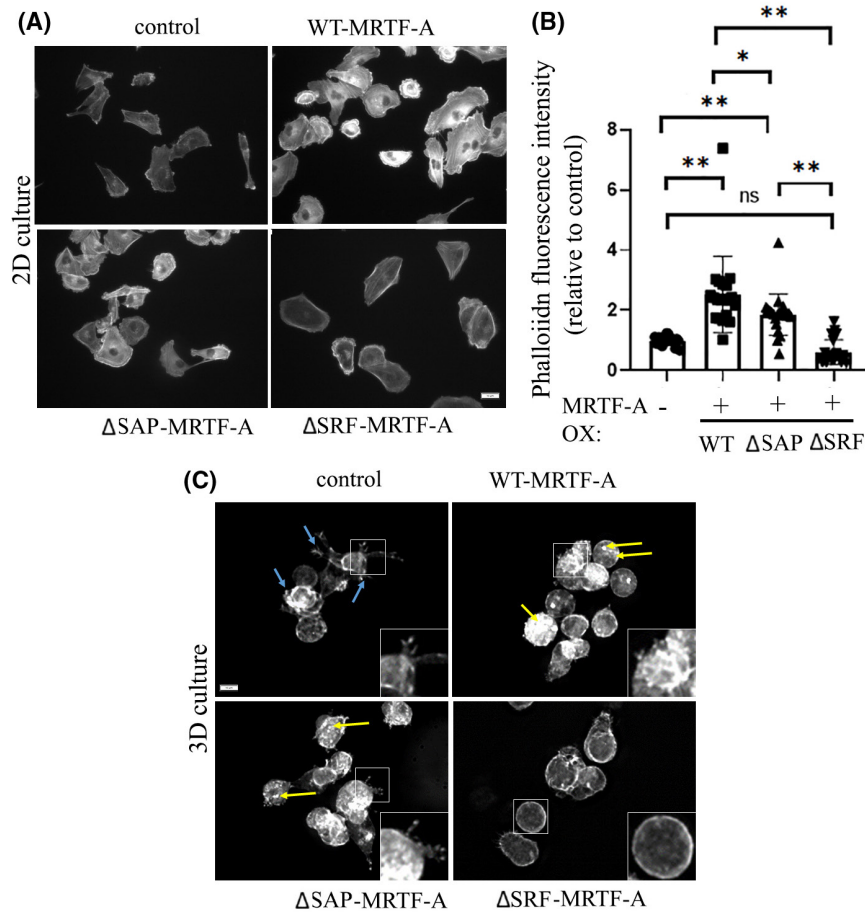
FIGURE 3 Effect of overexpression of wild-type versus functional mutants of MRTF-A on actin cytoskeleton in 2D and 3D cultures of MDA-231 cells. (A, B) Representative fluorescence images of phalloidin-stained cells (panel A; scale bar 10 μm) and quantification of phalloidin fluorescence intensity for the indicated groups in 2D culture. (C) Representative fluorescence images of phalloidin-stained cells of the indicated groups in 3D culture (blue arrow––FLP, yellow arrow––F-actin cluster). The insets show magnified images of the regions of interest outlined by squares
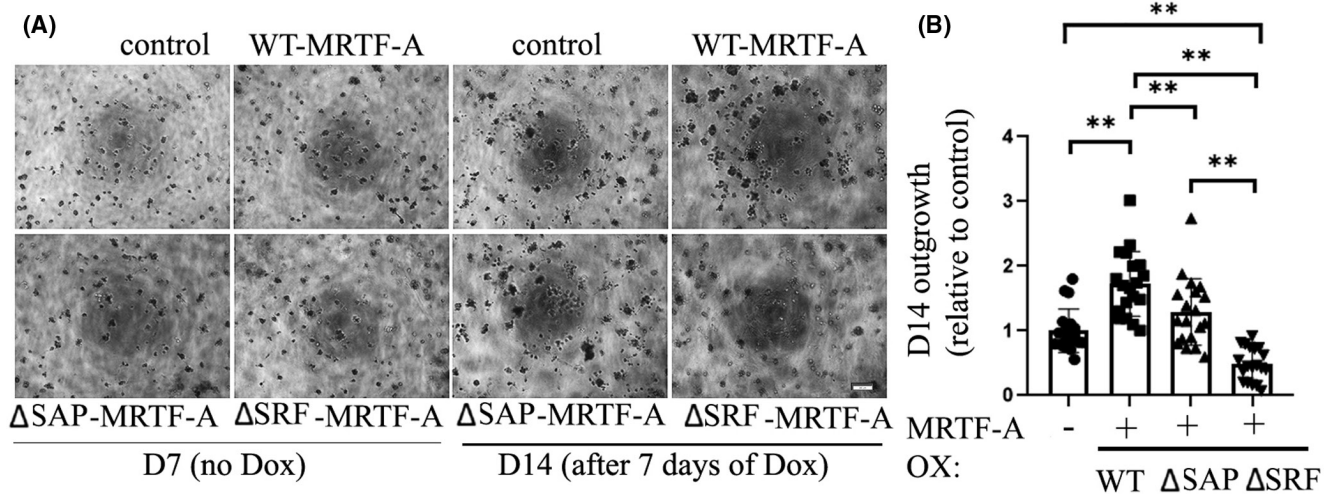

FIGURE 4 Effect of overexpression of wild-type versus functional mutants of MRTF-A on progression of pre-established outgrowth of breast cancer cells in MoT assay. Representative images (panel A) and quantification (panel B) of MoT outgrowth assays of the indicated cell lines subjected to either Dox-dependent induction of MRTF-A constructs. In these experiments, cells were allowed to outgrow for 7 days before Dox (to turn on expression of transgenes) was added to the culture for an additional 7 days and final outgrowth quantification on day 14. Data are summarized from three independent experiments (**$p < 0.01$). Values are presented as mean ± SD (**$p < 0.01$). Scale bar represents 200 μm

adaptation/metastatic seeding, we performed a second set of in vivo experiments to specifically query MRTF's role in post-seeding metastatic outgrowth of BC cells. In

these experiments, we inoculated tumor cells in the animals without prior induction of MRTF constructs and allowed sufficient time (7 days) for metastatic seeding to
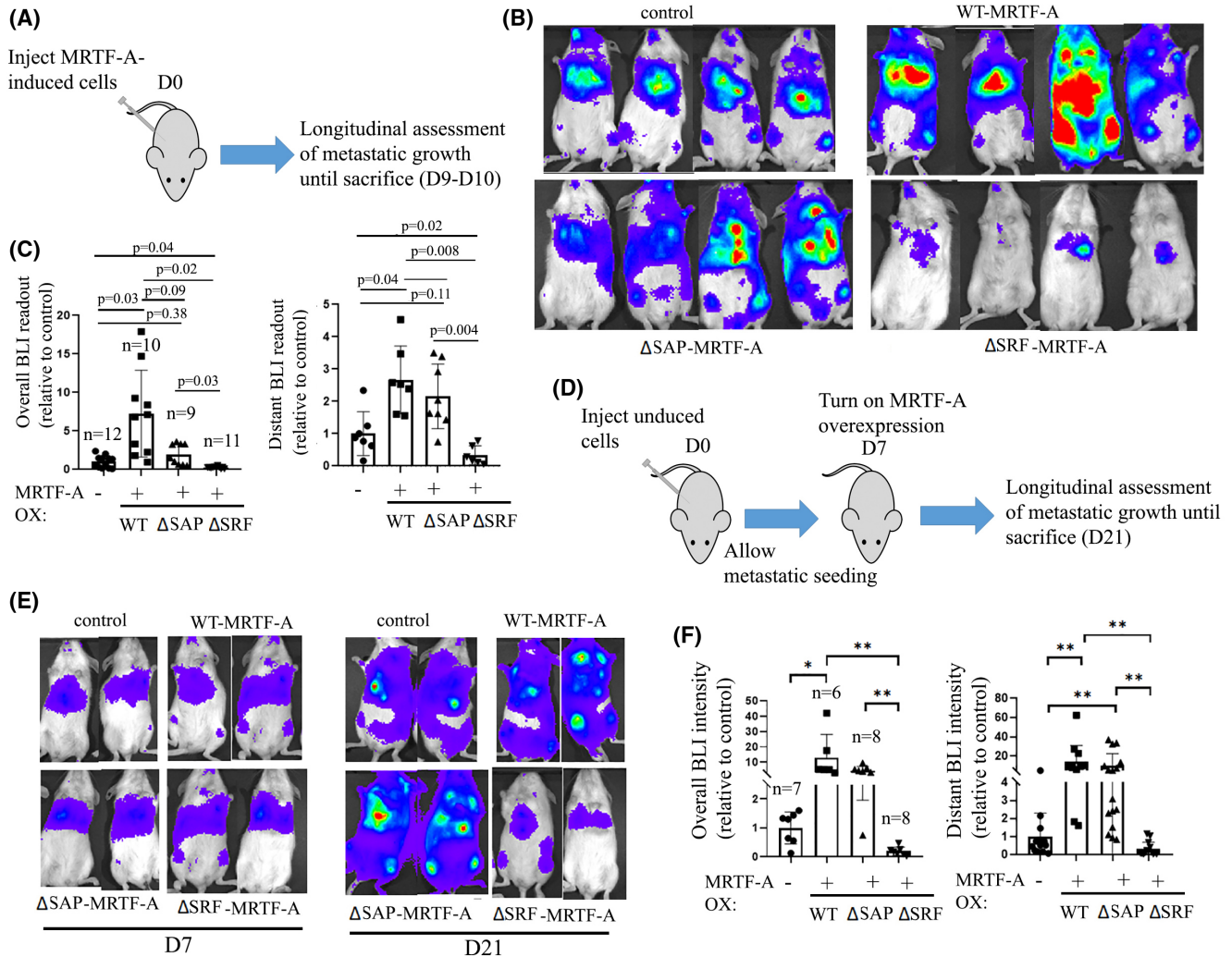
FIGURE 5 Effect of overexpression of WT versus functional mutants of MRTF-A on experimental metastasis of breast cancer cells. (A) Schematic representation of experimental metastasis experiments with pre-induced MRTF-A overexpressing MDA-231 cells in NSG mice. (B, C) Representative bioluminescence imaging (BLI) images (panel B) and quantification of BLI signal (overall and distant metastases— panel C) of NSG mice 8–10 days after intracardiac injection of MDA-231 cells overexpressing the indicated MRTF-A constructs ('n'—number of animal in each group pooled from three experiments) (**$p<0.01$). (D) Schematic representation of experimental metastasis experiments involving delayed induction of MRTF-A overexpression in post-inoculated MDA-231 cells in NSG mice. (E, F) Representative BLI images (panel E) and quantification of BLI signal (overall and distant metastases––panel F) of NSG mice 21 days after intracardiac injection of MDA-231 cells and 14 days after induction of the indicated MRTF-A constructs ('n'—number of animal in each group pooled from three experiments) (**$p<0.01$; *$p<0.05$). For scoring distant BLI readout, rectangular regions of interest were constructed in the head and lower extremity regions of the animals and cumulative BLI signals in those regions were obtained

occur before turning on and maintaining the transgene expression by DOX exposure and longitudinal follow-up of development of metastases by BLI until sacrifice (day 21) as schematized in Figure 5D. As expected, our experimental metastasis assay revealed comparable BLI readout for all four group of animals on day 7 prior to DOX exposure, which further suggested no leaky transgene expression in vivo without the presence of DOX (Figure 5E). The end-point BLI (both overall and distant) readouts of animals inoculated with WT-MRTF-A and ΔSAP-MRTF-A expressers were dramatically higher than those inoculated with either control or ΔSRF-MRTF-A expressing cells. No

statistically significant difference in BLI readout was evident between animals bearing WT-MRTF-A and ΔSAP-MRTF-A expressing cells (Figure 5F). These data further demonstrate critical importance of MRTF-SRF interaction in post-seeding metastatic outgrowth of BC cells.

To determine whether disruption of MRTF-SRF interaction has any effect on general tumorigenic ability of BC cells, we performed orthotopic xenograft experiments with the various sublines of MDA-231 cells. In these experiments, tumor cells were inoculated in uninduced condition, and after 10 days (thus allowing sufficient time for engraftment of tumor cells in the mammary gland),

animals were subjected to DOX-supplemented water treatment to trigger and maintain transgene expression. We found that overexpression of either WT-MRTF-A or ΔSAP-MRTF-A accelerated primary tumor growth relative to control group with the average tumor burden highest for those inoculated with WT-MRTF-A overexpressing cells. Immunoblot analyses of tumor lysates prepared from these animals confirmed mCherry expression (a marker co-expressed with MRTF-A) confirming transgene expression in vivo (Figure 6A). Note that the weak intensity of mCherry band in samples prepared from ΔSRF-MRTF-A expresser-inoculated tissue is due to severe defect in tumor formation in this group of animals. Animals injected with ΔSRF-MRTF-A expressers either failed to form palpable tumor or formed tumors of negligible size (Figure 6B,C). Collectively, our data demonstrate that disruption of MRTF-SRF interaction critically impairs the general tumorigenic ability of BC cells regardless of primary versus metastatic site.

3.4 | MRTF-targeting small molecule suppresses outgrowth aggressiveness of BC cells in vitro and metastatic colonization in vivo

We next asked whether development of metastases from circulating tumor cells is susceptible to pharmacological intervention of MRTF/SRF signaling. Small molecule CCG-1423 or its structural analogs (e.g., CCG-203971) bind to the inhibitory actin-binding RPEL motifs of MRTFs preventing their nuclear import and transcriptional activity.[30] Although CCG-series compounds also target other RPEL-domain bearing proteins, such as MICAL (a redox-sensitive actin-regulatory protein)[31] and pirin (an iron-dependent co-transcription factor,[32] these are the only available and widely used pharmacological tools to inhibit MRTF/SRF signaling. In our previous study, we established that CCG-1423, when used at 10 µM concentration in 2D cell culture, causes profound inhibition of cellular MRTF function in MDA-231 and endothelial cells (as judged by the extent of reduction of SRF level as expected from SRF being a transcriptional target of MRTF/SRF complex) without compromising cell viability.[33] Given our experimental data suggesting MRTF-dependency for outgrowth of both ER+ and ER- BC cells, we assessed the effect of addition of either 10 µM CCG-1423 or in some experiments, 25 µM concentration of CCG-203971 (a concentration that has been previously used in other studies [[34,35]]) on single-cell outgrowth of a range of BC cells spanning different molecular subtypes in MoT assays. Treatment with equivalent concentration of DMSO served as negative control. These studies were performed with a total of eight different cell lines representing different molecular subtypes of BC, which included two human luminal-A (MCF7 and T47D), two human Her2+ (BT-474 and SKBR3), two human metastatic TNBC (MDA-231 and MDA-468), and two murine metastatic TNBC (4T1 and D2A1) cell lines. Similar to the effect of MRTF KD, treatment of CCG compound also led to growth arrest of many cells at a single-cell stage dramatically reducing the overall outgrowth of all eight BC cell lines (Figures 7A,B; Figure S3). By live/dead staining, we
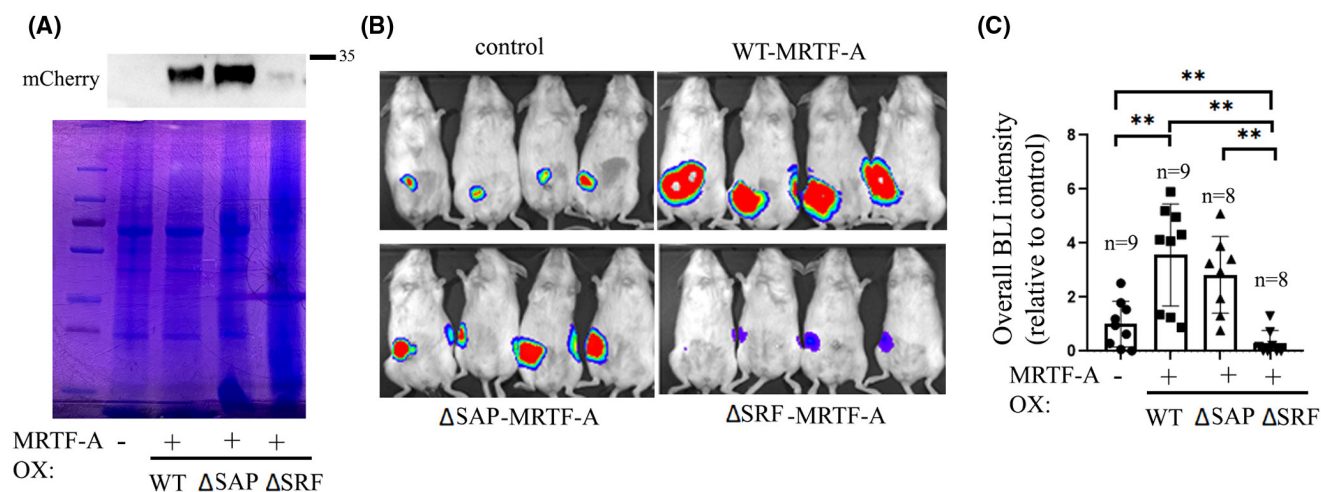

FIGURE 6 Effect of overexpression of WT versus functional mutants of MRTF-A on primary tumor forming ability of breast cancer cells. (A) Immunoblot of mammary tumor lysates showing DOX-induced expression of mCherry (a reporter co-expressed with MRTF-A) in vivo from orthotopic xenograft experiments with the indicated MDA-231 sublines (Coomassie staining of lysates serves as loading control). (B, C) Representative bioluminescence imaging (BLI) images (panel B) and quantification of the overall BLI signal (panel C) demonstrating relative tumor growth in various groups of animals ~30 days after tumor cell inoculation. Cells were induced to overexpress the indicated MRTF-A constructs 10 days after the initial injection ('*n*'—number of animal in each group pooled from two experiments) (**$p < 0.01$)
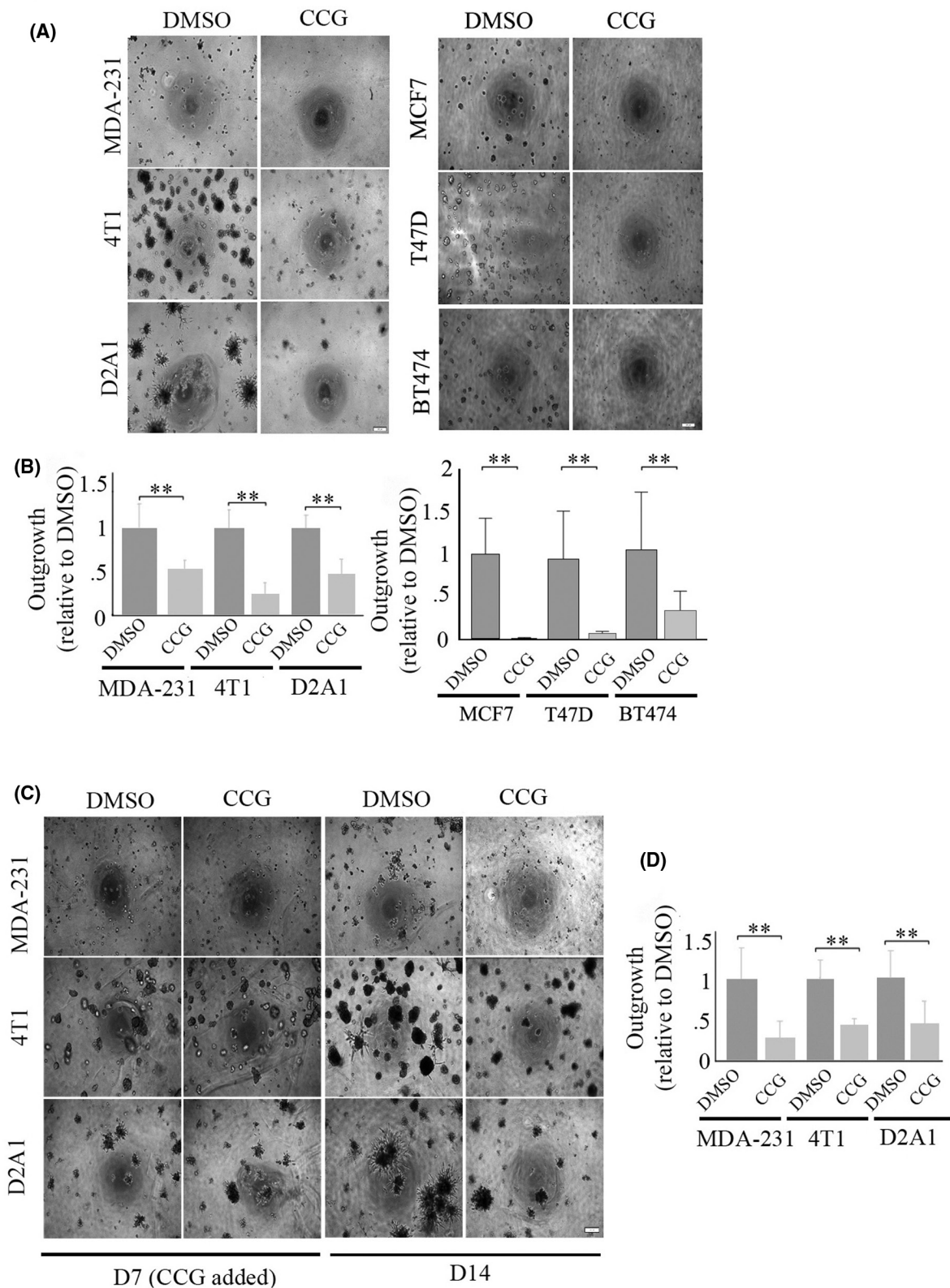
FIGURE 7 Effect of the treatment of CCG compounds on single-cell outgrowth and progression of established outgrowth of breast cancer (BC) cells in MoT assay. (A, B) Representative images (panel A) and quantifications (panel B) of single-cell outgrowth of the indicated BC cell lines treated with either DMSO (vehicle control) or CCG compound (either 25 μM CCG-203971 or 10 μM CCG-1423) in MoT assays. (C, D) Representative images of outgrowth progression of the indicated BC cell lines on days 7 and 14 in MoT cultures (panel C). The colonies were allowed to form for 7 days in regular culture media before cultures were treated with either DMSO or 25 μM CCG-203971 for an additional 7 days. Panel D summarizes the outgrowth of CCG-treated cultures relative to DMSO control for each cell type. All data summarized from three independent experiments (**$p < 0.01$). Values are presented as mean ± SD. Scale bar represents 200 μm

confirmed that CCG compound did not compromise cell viability in either 2D or 3D culture suggesting that reduced 3D outgrowth of BC cells in CCG compound-treatment setting is primarily due to proliferation arrest (Figure S4A–C). By qRT-PCR and/or immunoblot analyses of 3D culture extracts, we a priori confirmed CCG-induced reduction in the expression of connective tissue growth factor (CTGF––a bonafide MRTF/SRF-target gene) in MDA-231 and 4T1 cells as an indicator for inhibition of MRTF function (Figure S4D,E). We also tested the effect of CCG-compound on the progression of pre-established outgrowth of three different BC cell lines including MDA-231, D2A1, and 4T1. Essentially, in these experiments, we allowed single-cell outgrowth for 7 days and then treated those cells with either CCG compound or DMSO for an additional 7 days before the end-point evaluation of the overall outgrowth. Consistent with the overexpression data, these experiments revealed that treatment of the CCG compound dramatically retards the progression of established outgrowth for all three BC cell lines (Figure 7C,D), indicating that progressive growth of BC cells is also susceptible to small molecules targeting of MRTF.

Finally, to determine the effect of small molecule inhibition of MRTF on metastatic colonization of BC cells in vivo, we performed experimental metastasis assay involving ICI of luc/GFP+4T1 TNBC cells in syngeneic Balb/c mice. Since immune cells play critical role in conditioning pre-metastatic niche to either restrict or favor metastatic colonization of tumor cells,[36] choosing 4T1 cells as our model system allowed us to investigate the effect of MRTF inhibition on metastatic outgrowth of TNBC cells in a fully immunocompetent background. In our experiments, mice inoculated with tumor cells were treated daily with intraperitoneal injection of either CCG-1423 or DMSO (as vehicle control) until their sacrifice (~10 days). Percentage of mice with distant metastasis (most prominent in bone) in DMSO treated group (9 out of 11––equivalent to 82%) was significantly higher than that belonging to the CCG-1423-treated group (4 out 11––equivalent to 36%) (Figure 8A). The average value of the overall endpoint BLI signal was higher in mice treated with DMSO than those subjected to CCG-1423 treatment (Figure 8B). Bone histology of BLI signal-positive bones further validated the presence of metastases (Figure 8C). These data provide a proof-of-principle of the pharmacological intervention of MRTF as an effective strategy to reduce metastatic colonization of BC cells.

4 | DISCUSSION

In the present study, we demonstrate that MRTF promotes outgrowth initiation and progression, and metastatic colonization of BC cells, and inhibiting MRTF function, either by suppressing its expression or pharmacological intervention, induces a dormancy-like phenotype in BC cells. Through our in vivo experiments in the setting of delayed induction of MRTF-A overexpression, we for the first time demonstrate that post-seeding metastatic outgrowth is critically dependent on MRTF-SRF interaction elucidating the underlying mechanism of impaired metastatic colonization of MRTF-deficient BC cells as previously reported by another group.[17] Severe impairment in primary tumor-forming ability of BC cells as a result of overexpression of ΔSRF-MRTF-A further suggest critical importance for MRTF-SRF interaction for general tumorigenic ability of BC cells regardless of primary versus metastatic site.

Initial post-extravasation survival of BC cells in a foreign tissue environment is also a critical determinant for metastatic colonization and a previous study showed that endothelial cells undergo increased apoptosis upon SRF depletion in vivo.[37] Overexpression of ΔSRF-MRTF-A is not molecular equivalent to total loss of either MRTF or SRF expression––this is further exemplified by defect in primary tumor formation of ΔSRF-MRTF-A overexpressing MDA-231 cells in our study versus no effect of either MRTF or SRF depletion on primary tumor forming ability of MDA-231 cells as reported previously.[17] Although disruption of MRTF-SRF interaction does not induce cell death in vitro, and delayed induction experiments specifically bypass the initial survival phase, we cannot absolutely rule out the possibility of tumor cell survival in a foreign tissue microenvironment being augmented by MRTF's action in an SRF-dependent manner. There are also several interesting but not mutually exclusive possibilities of how disruption of MRTF-SRF interaction impairs metastatic colonization of BC cells. The most intuitive explanation is that a subset of MRTF/SRF-target genes with pro-proliferative and/or pro-survival actions are directly responsible for promoting metastatic outgrowth. However, since TCF is an antagonist of MRTF-dependent SRF-target gene expression,[22] disruption of MRTF-SRF interaction could hyperactivate the TCF-SRF gene regulatory pathway. Although TCF's action generally promotes cell proliferation, induction of cell-cycle arrest/senescence in tumor cells upon encountering excessive proliferation signal is not uncommon. Another possibility is that blockade of MRTF-SRF interaction indirectly suppresses tumor cell outgrowth by favoring MRTF's ability to interact with other transcription factors that have tumor-suppressive functions (e.g., SMADs). Furthermore, since our experiments were performed in overexpression settings, we cannot completely ignore a scenario where disrupting SRF's interaction of MRTF might either indirectly favor SAP-domain-driven gene expression or block
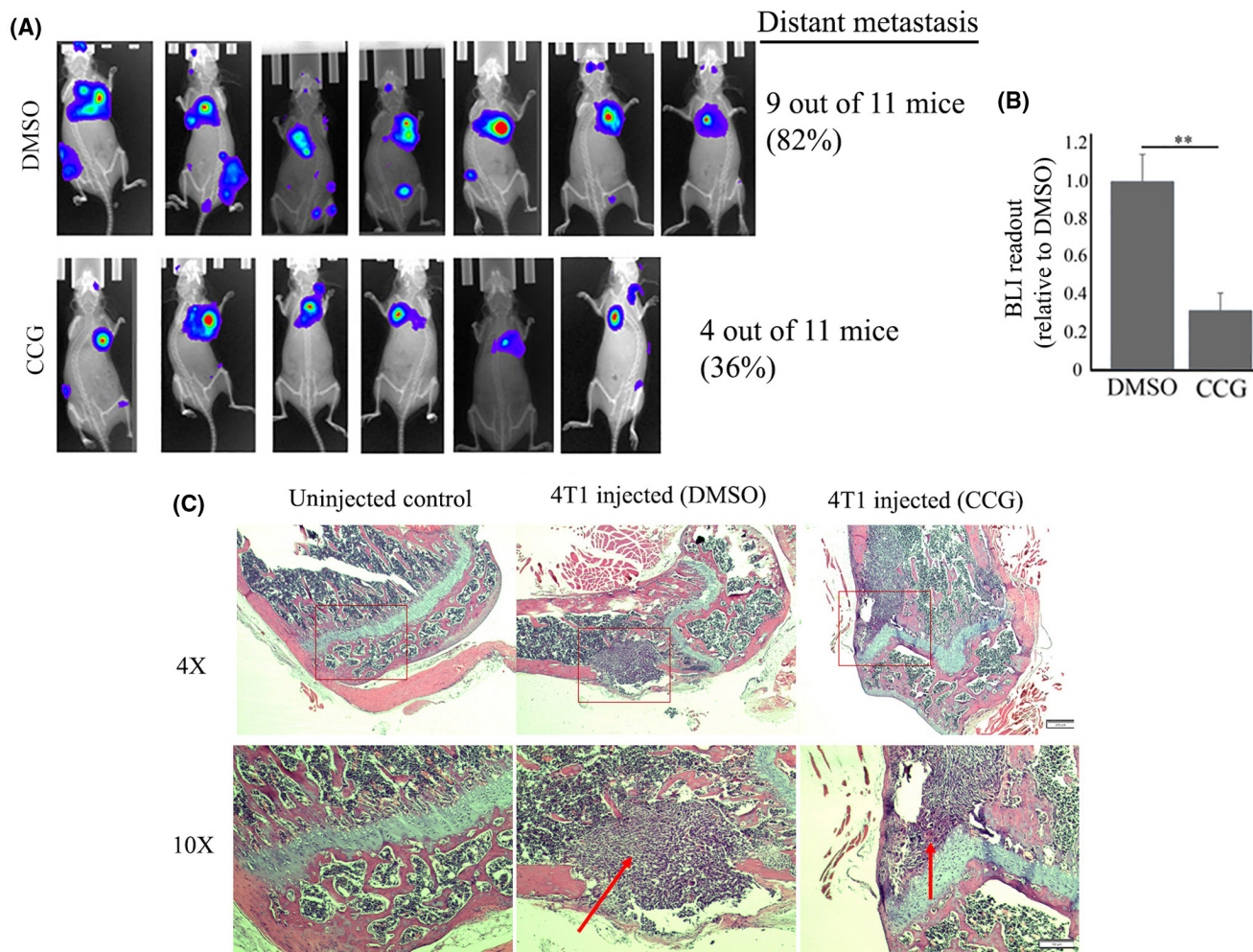
FIGURE 8 Effect of CCG-1423-treatment on experimental metastasis of 4T1-luc cells in syngeneic immunocompetent mice. (A, B) End-point bioluminescence images superimposed on X-ray images of 4T1-luc cells-administered Balb/c mice following daily intraperitoneal injection of either DMSO or CCG-1423; Images were taken 10 days after intracardiac injection of tumor cells. Quantification of end-point bioluminescence imaging (BLI) readout for the two groups pooled from three experiments are shown in panel B ($n = 11$ animals in each treatment group). (C) H&E staining of histosections of BLI signal-positive bones confirm presence of metastases (arrows); IHC of bone from mouse not injected with tumor cells is shown alongside for comparison. Scale bars for 4× and 10× represents 200 and 100 μm, respectively

transcription of a subset of genes that require both SAP-domain and SRF-related activities of MRTF-A thereby altering cancer cell phenotype. However, given that ΔSAP-MRTF-A expressers did not exhibit any defect in post-extravasation metastatic outgrowth in our studies, we speculate that the contribution of altered SAP-domain activity of MRTF, if at all, is minimal in conferring to the phenotype of ΔSRF-MRTF-A expressing cells. Future studies are needed to probe these different possibilities.

Previously demonstrated inhibition of experimental lung metastasis of melanoma cells by small molecule CCG-203971 (a derivative of the parent compound CCG-1423)[38] provided the first proof-of-concept for the utility of targeting MRTF/SRF pathway as a potential antimetastatic strategy. The present study focusing on BC cells not only extends the utility of CCG-series compound as

an antimetastatic agent to other types of cancer, but also addresses two important gaps. First, since the antimetastatic activity of CCG compound on melanoma cells was previously demonstrated in immunodeficient mice, whether interfering with MRTF signaling is also effective in inhibiting metastatic colonization of tumor cells in a fully intact immune background (a physiologically relevant scenario) remained unclear. Second, MRTF is also a highly mechanosensitive transcription factor. Soft substrates promote cytoplasmic sequestration of MRTF and conversely, stiff substrates drive nuclear accumulation of MRTF.[39] ECM stiffness plays a major role in dormancy-to-proliferation switch during metastatic outgrowth of cancer cells. Stiffer ECM substrates allow cancer cells to escape from dormancy fueling the metastatic growth.[40] Therefore, whether metastatic colonization of cancer cells

in mechanically rigid tissues is also susceptible to pharmacological inhibition of MRTF signaling was unclear. These two specific gaps were collectively addressed herein through demonstration of dramatic inhibition of experimental bone metastasis of BC cells by CCG-1423 in immunocompetent mice.

Metastatic outgrowth of extravasated BC cells is critically dependent upon early changes in actin cytoskeletal architecture marked by formation of F-actin-rich FLP and actin stress-fibers. These cytoskeletal structures enable activation of a proliferation-inducing signaling axis initiated by cell-ECM adhesion in disseminated BC cells leading to metastatic outgrowth. Failure to initiate FLP and actin stress-fibers assembly induces dormancy in disseminated BC cells in vitro and in vivo.[1,25,27,41] Correlated with the outgrowth results, we show that MRTF promotes actin assembly and formation of F-actin-based structures in BC cells. Actin-binding proteins which are either bonafide transcriptional targets of MRTF (e.g., mDia2)[42] or indirectly regulated downstream of MRTF activity (e.g., profilin)[26] play an important role in actin-based structure formation and metastatic colonization of BC cells. Therefore, it will be interesting to determine in the future whether MRTF regulates dormancy-emergence behavior of BC cells partly through actin cytoskeletal modulation. Finally, our studies showed that in addition to impairing single-cell outgrowth, CCG treatment significantly dampened the progression of established outgrowth of BC cells in vitro, consistent with our findings in MRTF-overexpression setting. Given that halting and/or reversing of an already progressive metastatic growth of tumor cells is challenging and an unmet clinical need, it is tempting to speculate that CCG treatment, either alone or in combination with chemotherapeutic drugs, could be a potential avenue to halt or regress established metastases and prolong survival in vivo, which needs to be examined in future studies.

CONFLICT OF INTEREST
The authors declare that the authors have no conflict of interest with the content of the article.

AUTHOR CONTRIBUTIONS
David Gau performed experiments, analyzed data, and wrote the manuscript, Pooja Chawla and Ian Eder performed experiments and analyzed data, Partha Roy wrote the manuscript and conceived the project.

ORCID
Partha Roy https://orcid.org/0000-0002-4946-8531

REFERENCES

1. Shibue T, Weinberg RA. Metastatic colonization: settlement, adaptation and propagation of tumor cells in a foreign tissue environment. *Semin Cancer Biol*. 2011;21:99-106.

2. Engers R, Gabbert HE. Mechanisms of tumor metastasis: cell biological aspects and clinical implications. *J Cancer Res Clin Oncol*. 2000;126:682-692.

3. Olson EN, Nordheim A. Linking Actin dynamics and gene transcription to drive cellular motile functions. *Nat Rev Mol Cell Biol*. 2010;11:353-365.

4. Gasparics A, Sebe A. MRTFs- master regulators of EMT. *Dev Dyn*. 2018;247:396-404.

5. Hendzel MJ. The F-act's of nuclear Actin. *Curr Opin Cell Biol*. 2014;28:84-89.

6. Gau D, Roy P. SRF'ing and SAP'ing—the role of MRTF proteins in cell migration. *J Cell Sci*. 2018;131:jcs218222.

7. Miralles F, Posern G, Zaromytidou AI, Treisman R. Actin dynamics control SRF activity by regulation of its coactivator MAL. *Cell*. 2003;113:329-342.

8. Posern G, Miralles F, Guettler S, Treisman R. Mutant actins that stabilise F-Actin use distinct mechanisms to activate the SRF coactivator MAL. *EMBO J*. 2004;23:3973-3983.

9. Vartiainen MK, Guettler S, Larijani B, Treisman R. Nuclear Actin regulates dynamic subcellular localization and activity of the SRF cofactor MAL. *Science*. 2007;316:1749-1752.

10. Mouilleron S, Guettler S, Langer CA, Treisman R, McDonald NQ. Molecular basis for G-Actin binding to RPEL motifs from the serum response factor coactivator MAL. *EMBO J*. 2008;27:3198-3208.

11. Muehlich S, Wang R, Lee SM, Lewis TC, Dai C, Prywes R. Serum-induced phosphorylation of the serum response factor coactivator MKL1 by the extracellular signal-regulated kinase 1/2 pathway inhibits its nuclear localization. *Mol Cell Biol*. 2008;28:6302-6313.

12. Cen B, Selvaraj A, Burgess RC, et al. Megakaryoblastic leukemia 1, a potent transcriptional coactivator for serum response factor (SRF), is required for serum induction of SRF target genes. *Mol Cell Biol*. 2003;23:6597-6608.

13. Sun Y, Boyd K, Xu W, et al. Acute myeloid leukemia-associated Mkl1 (Mrtf-a) is a key regulator of mammary gland function. *Mol Cell Biol*. 2006;26:5809-5826.

14. Sotiropoulos A, Gineitis D, Copeland J, Treisman R. Signal-regulated activation of serum response factor is mediated by changes in Actin dynamics. *Cell*. 1999;98:159-169.

15. Duggirala A, Kimura TE, Sala-Newby GB, et al. Camp-induced Actin cytoskeleton remodelling inhibits MKL1-dependent expression of the chemotactic and pro-proliferative factor, CCN1. *J Mol Cell Cardiol*. 2015;79:157-168.

16. Seifert A, Posern G. Tightly controlled MRTF-A activity regulates epithelial differentiation during formation of mammary acini. *Breast Cancer Res*. 2017;19:68.

17. Medjkane S, Perez-Sanchez C, Gaggioli C, Sahai E, Treisman R. Myocardin-related transcription factors and SRF are required for cytoskeletal dynamics and experimental metastasis. *Nat Cell Biol*. 2009;11:257-268.

18. Er EE, Valiente M, Ganesh K, et al. Pericyte-like spreading by disseminated cancer cells activates YAP and MRTF for metastatic colonization. *Nat Cell Biol*. 2018;20:966-978.

19. Tello-Lafoz M, Srpan K, Sanchez EE, et al. Cytotoxic lymphocytes target characteristic biophysical vulnerabilities in cancer. *Immunity*. 2021;54:1037-1054.e1037.

20. Asparuhova MB, Secondini C, Ruegg C, Chiquet-Ehrismann R. Mechanism of irradiation-induced mammary cancer metastasis: a role for SAP-dependent Mkl1 signaling. *Molecular Oncology*. 2015;9:1510-1527.

21. Gurbuz I, Ferralli J, Roloff T, Chiquet-Ehrismann R, Asparuhova MB. SAP domain-dependent Mkl1 signaling stimulates proliferation and cell migration by induction of a distinct gene set indicative of poor prognosis in breast cancer patients. *Mol Cancer*. 2014;13:22.

22. Gualdrini F, Esnault C, Horswell S, Stewart A, Matthews N, Treisman R. SRF co-factors control the balance between cell proliferation and contractility. *Mol Cell*. 2016;64:1048-1061.

23. Barkan D, Green JE. An in vitro system to study tumor dormancy and the switch to metastatic growth. *J Vis Exp*. 2011;2914.

24. Shibue T, Brooks MW, Inan MF, Reinhardt F, Weinberg RA. The outgrowth of micrometastases is enabled by the formation of filopodium-like protrusions. *Cancer Discov*. 2012;2:706-721.

25. Shibue T, Weinberg RA. Integrin beta1-focal adhesion kinase signaling directs the proliferation of metastatic cancer cells disseminated in the lungs. *Proc Natl Acad Sci USA*. 2009;106:10290-10295.

26. Joy M, Gau D, Castellucci N, Prywes R, Roy P. The myocardin-related transcription factor MKL co-regulates the cellular levels of two profilin isoforms. *J Biol Chem*. 2017;292:11777-11791.

27. Barkan D, Kleinman H, Simmons JL, et al. Inhibition of metastatic outgrowth from single dormant tumor cells by targeting the cytoskeleton. *Cancer Res*. 2008;68:6241-6250.

28. Barkan D, Green JE, Chambers AF. Extracellular matrix: a gatekeeper in the transition from dormancy to metastatic growth. *Eur J Cancer*. 2010;46:1181-1188.

29. El Touny LH, Vieira A, Mendoza A, Khanna C, Hoenerhoff MJ, Green JE. Combined SFK/MEK inhibition prevents metastatic outgrowth of dormant tumor cells. *J Clin Investig*. 2014;124:156-168.

30. Hayashi K, Watanabe B, Nakagawa Y, Minami S, Morita T. RPEL proteins are the molecular targets for CCG-1423, an inhibitor of rho signaling. *PLoS One*. 2014;9:e89016.

31. Lundquist MR, Storaska AJ, Liu TC, et al. Redox modification of nuclear Actin by MICAL-2 regulates SRF signaling. *Cell*. 2014;156:563-576.

32. Lisabeth EM, Kahl D, Gopallawa I, et al. Identification of Pirin as a molecular target of the CCG-1423/CCG-203971 series of antifibrotic and antimetastatic compounds. *ACS Pharmacol Transl Sci*. 2019;2:92-100.

33. Gau D, Veon W, Capasso TL, et al. Pharmacological intervention of MKL/SRF signaling by CCG-1423 impedes endothelial cell migration and angiogenesis. *Angiogenesis*. 2017;20:663-672.

34. Yu-Wai-Man C, Spencer-Dene B, Lee RMH, et al. Local delivery of novel MRTF/SRF inhibitors prevents scar tissue formation in a preclinical model of fibrosis. *Sci Rep*. 2017;7:518.

35. Johnson LA, Rodansky ES, Haak AJ, Larsen SD, Neubig RR, Higgins PD. Novel rho/MRTF/SRF inhibitors block matrix-stiffness and TGF-beta-induced fibrogenesis in human colonic myofibroblasts. *Inflamm Bowel Dis*. 2014;20:154-165.

36. Doglioni G, Parik S, Fendt SM. Interactions in the (pre)metastatic niche support metastasis formation. *Front Oncol*. 2019;9:219.

37. Weinl C, Riehle H, Park D, et al. Endothelial SRF/MRTF ablation causes vascular disease phenotypes in murine retinae. *J Clin Invest*. 2013;123:2193-2206.

38. Haak AJ, Appleton KM, Lisabeth EM, et al. Pharmacological inhibition of Myocardin-related transcription factor pathway blocks lung metastases of RhoC-overexpressing melanoma. *Mol Cancer Ther*. 2017;16:193-204.

39. Foster CT, Gualdrini F, Treisman R. Mutual dependence of the MRTF-SRF and YAP-TEAD pathways in cancer-associated fibroblasts is indirect and mediated by cytoskeletal dynamics. *Genes Dev*. 2017;31:2361-2375.

40. Barkan D, El Touny LH, Michalowski AM, et al. Metastatic growth from dormant cells induced by a col-I-enriched fibrotic environment. *Cancer Res*. 2010;70:5706-5716.

41. Shibue T, Brooks MW, Weinberg RA. An integrin-linked machinery of cytoskeletal regulation that enables experimental tumor initiation and metastatic colonization. *Cancer Cell*. 2013;24:481-498.

42. Sun Q, Chen G, Streb JW, et al. Defining the mammalian CArGome. *Genome Res*. 2006;16:197-207.

SUPPORTING INFORMATION

Additional supporting information may be found in the online version of the article at the publisher's website.